

# Linear Stability of the Confined Compressible Reacting Mixing Layer

D. S. Shin\* and J. H. Ferziger†  
Stanford University, Stanford, California 94305

This paper investigates the linear stability of confined mixing layers with special emphasis on the effects of heat release and compressibility. The results show that reflection of supersonic disturbances by the walls makes the confined supersonic mixing layer more unstable than the unconfined free shear layer. Decreasing the distance between the walls makes the flow more unstable. However, subsonic disturbances are relatively unaffected by the walls. Heat release and Mach number hardly change the growth rates of supersonic disturbances. The most unstable supersonic disturbances are two-dimensional in rectangular channel flows, but three-dimensional in partially confined flows. Finally, the reactants are not strongly mixed by supersonic instabilities, which mainly disturb one side of the layer.

## Nomenclature

$B$	= breadth of the rectangular channel
$c_r$	= real part of the wave velocity
$F$	= general dependent variable
$\bar{F}$	= mean of a general dependent variable
$F'$	= fluctuation of a general dependent variable
$\hat{F}$	= eigenfunction of general dependent variable
$H$	= half of the channel height
$M_1$	= Mach number of the upper stream
$M_2$	= Mach number of the lower stream
$M_c$	= convective Mach number
$M_r$	= relative Mach number
$m$	= spanwise wave number
$p$	= pressure
$[RXN1],$ $[RXN2]$	= density variation terms in the stability equation
$T$	= temperature
$T_{ad}$	= nondimensional adiabatic flame temperature
$t$	= time
$u$	= velocity component in the $x$ direction
$v$	= velocity component in the $y$ direction
$w$	= velocity component in the $z$ direction
$x$	= streamwise coordinate
$y$	= normal coordinate
$y_i$	= mass fraction of the $i$ th species
$z$	= spanwise coordinate
$\alpha$	= streamwise wave number
$\alpha_i$	= imaginary part of the streamwise wave number
$\gamma$	= specific heat ratio
$\theta$	= propagation angle of disturbance
$\mu$	= Mach angle
$\rho$	= density
$\omega$	= frequency

## Subscripts

$F$	= fuel
$O$	= oxidizer

## I. Introduction

REACTING free shear layers occur in many systems, including gas turbine combustors and rockets. Chemical reaction can occur only when the reactants are molecularly mixed. However, short residence times require efficient mixing between the fuel and oxidizer. This is especially important in air-breathing ramjets. Fast mixing requires the flow to be vigorously turbulent, which requires the laminar flow to be unstable. Hence, understanding of the stability characteristics of reacting free shear layers may lead to techniques for enhancing mixing or controlling the flow. Stability analysis can also predict some characteristics of the turbulent reacting mixing layer. The conclusions may be expected to apply, with quantitative modifications, to other shear flows, e.g., jets.

Most stability analyses of supersonic mixing layers have considered unconfined shear layers.<sup>1-6</sup> However, the supersonic mixing layers in ramjet combustors and most experiments are confined by solid walls. Two distinct types of instabilities may occur in confined shear layers. One is the Kelvin-Helmholtz instability found in subsonic shear layers; the other is the supersonic instability. In low-speed flows, the effects of walls on the Kelvin-Helmholtz instability are relatively small so long as they are separated by many shear layer thicknesses. However, in high-speed flows, some of the energy of the acoustic radiation that would leave an infinite system is reflected from the walls. This reflection can alter the stability characteristics of the flow significantly.<sup>7-10</sup>

To include the effect of chemical reaction, we shall consider a reacting mixing layer in a channel. The chemistry model is a finite-rate, single-step, irreversible reaction with Arrhenius kinetics. At the walls, we could apply no-slip boundary conditions. However, the focus of this study is on the shear layer, and the wall boundary layers are not important so long as they are much thinner than the shear layer and channel width. Hence, we allow fluid slip at the walls but no penetration. Furthermore, heat loss and chemical reaction at the walls are excluded. Laminar flows obtained by solving the compressible boundary-layer equations with slip-wall boundary conditions are used as the basis for the stability study because the confining walls hardly change the profiles of laminar flows.<sup>11</sup> All flow variables are nondimensionalized by their fast-stream values.

We shall consider the effects of heat release, Mach number, frequency, wave number, thickness of shear layer, as well as distance between walls and direction of propagation of the disturbance waves. We use nondimensional adiabatic flame temperature  $T_{ad}$  to express the amount of heat release from combustion. Note that for a given  $T_{ad}$ , the actual temperature rise in high Mach number flows may be higher than that of

Received March 24, 1992; revision received July 4, 1992; accepted for publication July 15, 1992. Copyright © 1992 by the American Institute of Aeronautics and Astronautics, Inc. All rights reserved.

\*Graduate Research Assistant, Thermosciences Division, Department of Mechanical Engineering; currently, Visiting Researcher, Mechanical Engineering Laboratory, Daikin Industries, Ltd., 1304, Kanaoka-cho, Sakai, Osaka 591, Japan.

†Professor, Thermosciences Division, Department of Mechanical Engineering. Member AIAA.

low Mach number flows because of viscous dissipation. How best to express the temperature rise from the combustion and viscous dissipation in a single parameter is still an open question.

## II. Inviscid Linear Stability Equation

We consider a spatially developing plane mixing layer in which the fuel and oxidizer are initially unmixed. The flow is confined to a rectangular channel of height  $2H$  and breadth  $B$  (see Fig. 1). We assume locally parallel mean flow and small wavelike disturbances propagating in the  $x$  direction. Each dimensionless quantity can be expressed as

$$F(x, y, z, t) = \bar{F}(y) + F'(x, y, z, t) \quad (1)$$

where  $\bar{F}(y)$  is the mean flow quantity and  $F'$  is the disturbance.

At the walls, we apply slip boundary conditions in accordance with laminar flows. Boundary conditions for the disturbances at the sidewalls ( $z = \pm B/2$ ) are, therefore,

$$\frac{\partial u'}{\partial z} = \frac{\partial v'}{\partial z} = w' = \frac{\partial \rho'}{\partial z} = \frac{\partial T'}{\partial z} = \frac{\partial p'}{\partial z} = \frac{\partial y_F'}{\partial z} = \frac{\partial y_O'}{\partial z} = 0 \quad (2)$$

Solutions for the disturbances that satisfy those boundary conditions are assumed to have the form

$$\begin{bmatrix} u' \\ v' \\ w' \\ \rho' \\ T' \\ p' \\ y_F' \\ y_O' \end{bmatrix} = \begin{bmatrix} \hat{u}(y) \cos(2m\pi z/B) \\ \hat{v}(y) \cos(2m\pi z/B) \\ \hat{w}(y) \sin(2m\pi z/B) \\ \hat{\rho}(y) \cos(2m\pi z/B) \\ \hat{T}(y) \cos(2m\pi z/B) \\ \hat{p}(y) \cos(2m\pi z/B) \\ \hat{y}_F(y) \cos(2m\pi z/B) \\ \hat{y}_O(y) \cos(2m\pi z/B) \end{bmatrix} e^{i(\alpha x - \omega t)} \quad (m = 0, 1, 2, \dots) \quad (3)$$

The perturbation equations are derived by linearizing the compressible Euler equations. Substituting Eq. (3) into the linearized governing equations, we derive a second-order ordinary differential equation for the pressure

$$\hat{p}'' - \left\{ \frac{2\alpha\hat{u}'}{(\alpha\hat{u} - \omega)} + \frac{\bar{\rho}}{\bar{T}}(\alpha\hat{u} - \omega)^2[RXN1] \right\} \hat{p}' - \left[ \alpha^2 + \left( \frac{2m\pi}{B} \right)^2 \right] - \gamma M_1^2(\alpha\hat{u} - \omega)^2 \left\{ \frac{1}{\bar{T}} + \frac{\bar{\rho}}{\bar{T}}[RXN2] \right\} \hat{p} = 0 \quad (4)$$

[RXN1] and [RXN2] are terms that represent the effect of density variation due to chemical reaction and compressibility on the instability; they are given in the previous paper.<sup>6</sup> The boundary conditions at the top and bottom walls become

$$\hat{p}'(H) = \hat{p}'(-H) = 0 \quad (5)$$

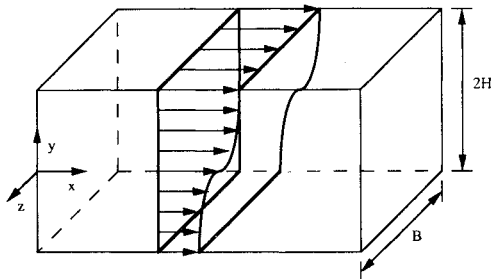


Fig. 1 Schematic diagram of spatially developing mixing layer in a rectangular channel.

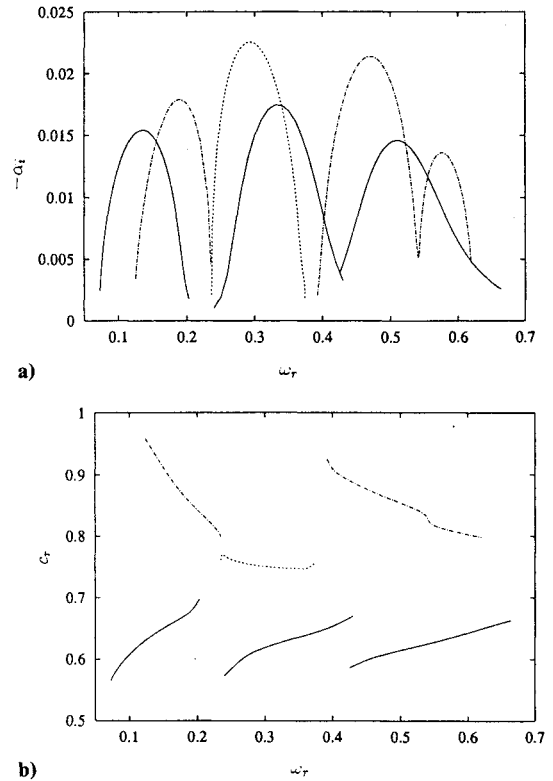


Fig. 2 Unstable modes: a) Amplification rates and b) phase velocities in supersonic relative Mach number;  $T_{ad} = 1$ ,  $M_1 = 6$ ,  $M_2 = 3$ ,  $m = 0$ ,  $H = 5$ ,  $\bar{T}_2 = 1$  (—, slow mode; ···, center mode; - · -, fast mode).

With these boundary conditions, Eq. (4) is solved by a combination of the shooting and Newton-Raphson methods.

## III. Results

### A. Effect of Walls

First, the effect of walls on the instability is examined. We begin by looking at the two-dimensional waves ( $m = 0$ ) in the nonreacting flow ( $T_{ad} = 1$ ) with  $H = 5$ . Because all length scales are nondimensionalized by initial vorticity thickness,  $H = 5$  means that wall separation is five times the vorticity thickness, which is small enough to permit interaction between the wall and unstable acoustic modes. When the Mach number of the disturbance relative to either freestream is supersonic ( $|M_r| > 1$ ), flows yield many supersonic unstable modes; these are similar to the supersonic modes found by Mack<sup>12</sup> in boundary layers. They arise from reflection of acoustic waves by the walls and do not exist in the absence of walls. Figure 2 shows the growth rates of these unstable modes and their phase velocities at  $M_1 = 6$  and  $M_2 = 3$ . There are additional unstable modes at higher frequencies; their amplification rates are lower. The unstable modes can be classified into the three families found in unconfined flows according to their phase speeds: center and two outer modes. The slow outer mode travels at lower speed than the center mode, whereas the fast outer mode travels at higher speed. The phase velocities of the fast modes decrease as the frequency increases, whereas those of slow modes increase with frequency. They appear to approach the average of the two freestream velocities. This behavior contrasts with what was found in unconfined flows, for which the phase velocities approach the freestream velocities. Each mode is unstable only over a relatively narrow frequency band. For this set of parameters, the most unstable mode is a center mode, but it is only slightly more unstable than one of the outer modes.

For the reacting flow with  $T_{ad} = 4$  and  $H = 5$ , when the relative Mach number is supersonic, three families of modes are unstable. Figure 3 shows the growth rates of these unstable

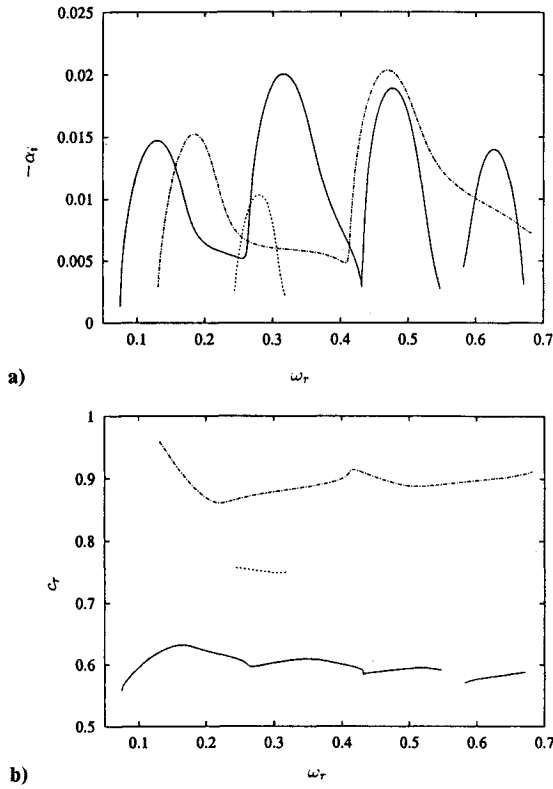


Fig. 3 Unstable modes: a) Amplification rates and b) phase velocities in supersonic relative Mach number;  $T_{ad} = 4$ ,  $M_1 = 6$ ,  $M_2 = 3$ ,  $m = 0$ ,  $H = 5$ ,  $\bar{T}_2 = 1$  (—, slow mode; ···, center mode; ---, fast mode).

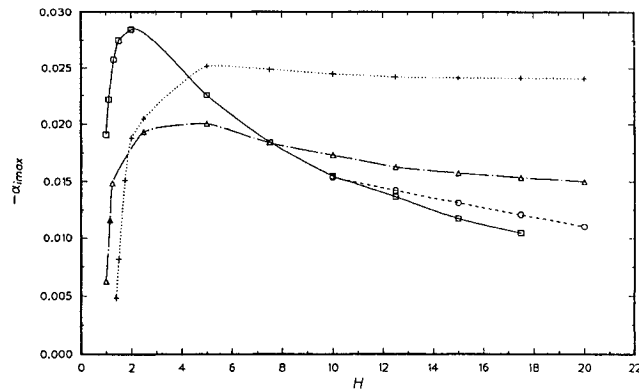


Fig. 4 Maximum amplification rates vs  $H$ ;  $m = 0$ ,  $M_1 = 6$ ,  $M_2 = 3$ ,  $\bar{T}_2 = 1$  ( $\square$ ,  $T_{ad} = 1$ , center mode;  $\circ$ ,  $T_{ad} = 1$ , slow mode;  $\Delta$ ,  $T_{ad} = 4$ , slow mode;  $+$ ,  $T_{ad} = 8$ , slow mode).

modes and the corresponding phase velocities for  $M_1 = 6$  and  $M_2 = 3$ . Other unstable modes with lower amplification rates and higher frequencies are not shown. The fast and slow modes have comparable amplification rates, whereas the center mode is less unstable. Unlike the situation in nonreacting flows, neither phase velocity approaches the average speed. Rather, the phase velocities of the outer modes appear to be almost independent of frequency.

Because the walls change the characteristics of supersonic unstable modes from those found in unconfined flows, the distance between the walls is an important parameter. For two-dimensional modes,  $m = 0$ , the growth rates are independent of the aspect ratio of the duct, i.e., the breadth has no effect on the stability. We calculated the properties of spatially growing waves at various values of  $H$  for fixed upper stream Mach number  $M_1$  and fixed mean velocity and temperature profiles. The instability behavior of the subsonic shear layer

hardly varies with the distance between the walls. However, the instability characteristics of supersonic shear layers change considerably as height increases. Figure 4 shows the maximum amplification rate as functions of  $H$  at  $M_1 = 6$  ( $M_2 = 3$ ). The smallest  $H$  considered is 1. For nonreacting flows, the most unstable modes are center modes when the walls are closely spaced ( $H \leq 10$ ). However, as the distance between the walls increases ( $H > 10$ ), slow modes become more unstable as in the unconfined flow cases. For reacting flows ( $T_{ad} = 4$  and 8), the most unstable modes are always slow modes. The maximum growth rates of both the nonreacting and reacting shear layers reach their maximum values and decrease as the distance between the walls decreases. The maximum growth rates occur about at  $H = 2$  for the nonreacting flow and about at  $H = 5$  for the reacting flows. As expected, reflection of acoustic waves by moderately closely spaced walls prevents radiation of energy and makes the flow more unstable. The effect is much larger in the nonreacting slow mode case for which the maximum growth rate at  $H = 5$  is about twice as large as that at  $H = 20$ . For  $T_{ad} = 4$ , the maximum growth rate at  $H = 5$  is about 1.4 times larger than that at  $H = 20$ . When  $H$  is relatively small ( $H < 4$ ), the nonreacting flow is more unstable than the reacting flows; the reverse is true for large  $H$  ( $H > 4$ ). Although the very closely spaced walls tend to make the flow less unstable than the moderately spaced walls, the real combustor will have a considerably large height and the effect will be small.

### B. Three-Dimensional Modes

In partially confined-channel flows, which have no side-walls, the disturbances are of the traveling-wave form in the transverse direction.<sup>6</sup> Figure 5 shows the geometry of the partially confined channel and rectangular channel. The only difference between partially confined flows and rectangular channel flows is the boundary condition at the side walls, Eq. (1). We studied the growth rate of three-dimensional modes in both types of flows. Because heat release favors two-dimensional instability, we considered only the nonreacting case ( $T_{ad} = 1$ ); because walls have little effect on the low-speed flow, only high-speed flows ( $M_1 = 6$ ,  $M_2 = 3$ ) were studied. Figure 6 shows the maximum amplification rates for various angles of propagation at  $H = 5$  for the case without sidewalls. Only the slow mode growth rates are given for readability; the fast mode growth rates are almost the same. The center mode is slightly more unstable than the outer modes at  $\theta = 0$  deg. As the angle increases, the center modes become less unstable. At large angles ( $\theta > 55$  deg), the center modes reappear and dominate, as in the unconfined flow<sup>6</sup>; they are subsonic relative to both freestreams. The most unstable center mode occurs at  $\theta = 70$  deg and the corresponding relative Mach number is 0.51; the amplification rate is slightly higher (about 8%) than that of the two-dimensional mode. The outer modes become more stable with increasing angle as in the unconfined flows. Thus, the behavior of partially confined flows is similar to that of unconfined flows, but the close spacing of the walls weakens the three-dimensionality.

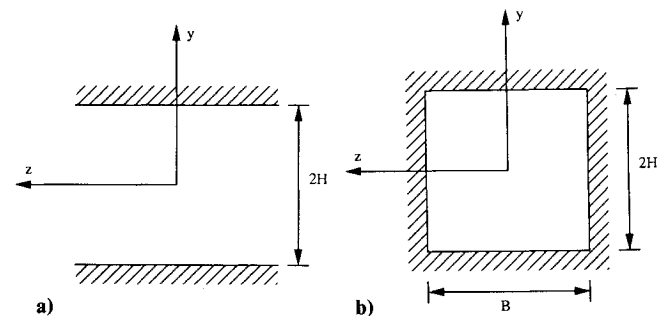


Fig. 5 Geometry of the a) partially confined channel and b) rectangular channel.

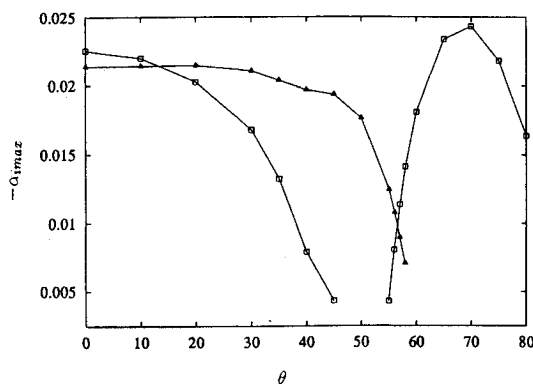
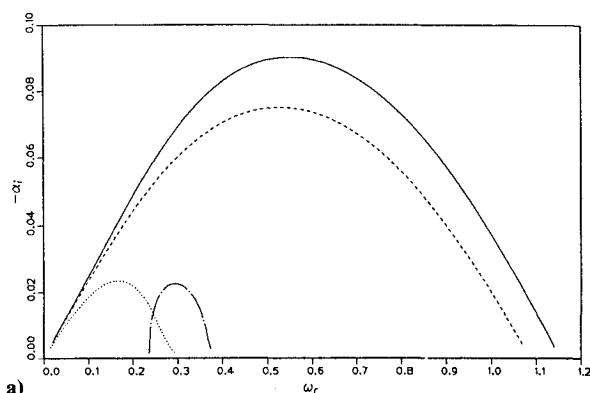
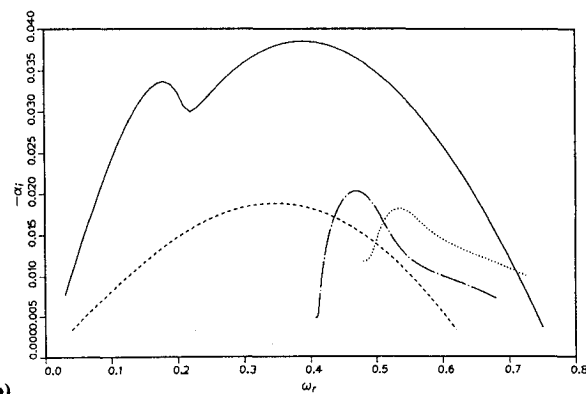


Fig. 6 Maximum growth rate vs obliqueness angle in partially confined flows at  $T_{ad} = 1$ ;  $\bar{T}_2 = 1$ ,  $M_1 = 6$ ,  $M_2 = 3$ ,  $H = 5$  ( $\square$ , center mode;  $\Delta$ , slow mode).



a)



b)

Fig. 7 Amplification rates in rectangular channel flow for a) nonreacting ( $T_{ad} = 1$ ) and b) reacting ( $T_{ad} = 4$ ) flows;  $B/2 = H = 5$ ,  $\bar{T}_2 = 1$  (—,  $M_1 = 2$ ,  $m = 0$ ; ----,  $M_1 = 2$ ,  $m = 1$ ; - · -,  $M_1 = 6$ ,  $m = 0$ ; ····,  $M_1 = 6$ ,  $m = 1$ ).

A rectangular channel might display three-dimensional instabilities due to reflections from the sidewalls. Because the transverse-boundary conditions [Eq. (1)] allow only integer values of the transverse wave number  $m$ , the three-dimensional modes in a rectangular channel are different from traveling modes in the transverse direction. We investigated the three-dimensional instability modes for both nonreacting ( $T_{ad} = 1$ ) and reacting ( $T_{ad} = 4$ ) rectangular-channel flows. Because a smaller distance between the walls makes the flow more unstable and the results with a larger distance agree well with unconfined flow cases, we chose 10 as the wall height. The breadth of the channel  $B$  was 10 in this study. We studied two different Mach numbers.  $M_1 = 2$  and 6 ( $M_2 = 1$  and 3); the first is considered a low-speed flow and the second a high-speed flow.

Figure 7a shows the amplification rates for the nonreacting cases. We consider only the center mode for nonreacting flows

( $T_{ad} = 1$ ) and the slow mode for reacting flows ( $T_{ad} = 4$ ), because they are the most unstable modes of the respective flows;  $m = 0$  corresponds to two-dimensional modes and  $m = 1$  to three-dimensional modes. We found only damped modes for  $m > 1$ . In the low-speed flow ( $M_1 = 2$ ), the three-dimensional mode ( $m = 1$ ) has lower amplification rates than the two-dimensional mode ( $m = 0$ ); this is similar to what we found for unconfined flows. In high-speed flows ( $M_1 = 6$ ), the three-dimensional mode ( $m = 1$ ) has lower amplification rates. This result shows that three-dimensional modes have lower amplification rates than two-dimensional modes in high-speed nonreacting flows, unlike unconfined or partially confined flows. Thus side walls favor two-dimensionality. However, it will be difficult to identify the large structures as two- and three-dimensional in experiments because the dominant unstable modes have comparable growth rates but various phase speeds, which is consistent with the present observation.<sup>13-15</sup> Figure 7b shows the results for the reacting cases. The most amplified modes are still two-dimensional ( $m = 0$ ), which is similar to the situation in unconfined reacting shear layers. As a consequence, we consider only two-dimensional modes below.

### C. Effect of Mach Number and Heat Release

This section studies the effect of the Mach number and heat release on the maximum growth rates of instabilities in confined shear layers. The wall height is fixed at 10. Figure 8 gives the maximum amplification rate vs the upper-stream Mach number and indicates that the maximum growth rate of the most unstable two-dimensional mode decreases with Mach number in both nonreacting ( $T_{ad} = 1$ ) and reacting ( $T_{ad} = 4$ ) flows. They appear to approach asymptotic values for  $M_1 > 4$  or  $M_c > 1$ , where  $M_c$  is the isentropic convective Mach number defined by Papamoschou and Roshko.<sup>16</sup>

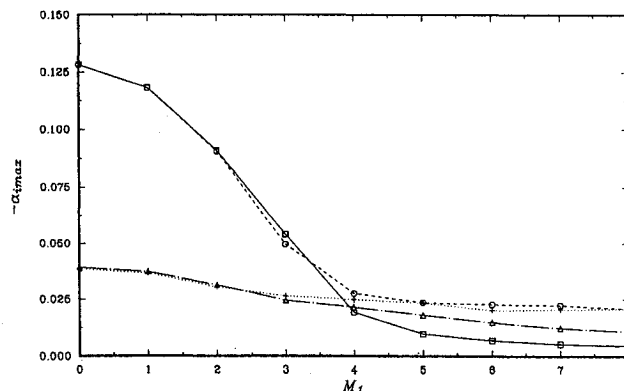


Fig. 8 Maximum amplification rates vs  $M_1$ ;  $m = 0$ ,  $H = 5$ ,  $\bar{T}_2 = 1$  ( $\square$ ,  $T_{ad} = 1$ , unconfined;  $\circ$ ,  $T_{ad} = 1$ , confined;  $\Delta$ ,  $T_{ad} = 4$ , unconfined; +,  $T_{ad} = 4$ , confined).

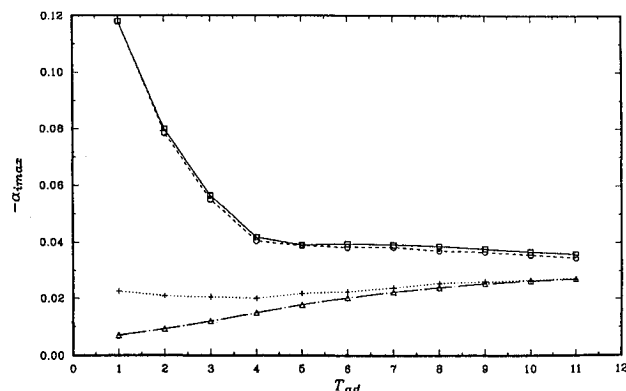


Fig. 9 Maximum amplification rates vs  $T_{ad}$ ;  $m = 0$ ,  $\bar{T}_2 = 1$  ( $\square$ ,  $M_1 = 1$ , unconfined;  $\circ$ ,  $M_1 = 1$ , confined,  $H = 5$ ;  $\Delta$ ,  $M_1 = 6$ , unconfined; +,  $M_1 = 6$ , confined,  $H = 5$ ).

In the nonreacting case, there is little difference between the unconfined and the confined flows when the isentropic convective Mach number is subsonic ( $M_1 < 4$ ). When the isentropic convective Mach number is supersonic ( $M_1 > 4$ ), reflection of acoustic waves by the walls makes the confined flow more unstable than the unconfined flow. At  $M_1 = 8$ , the maximum growth rate of the confined flow is about four times that of the unconfined flow. However, it is small (about 16%) compared to the growth rate of the cold flow at  $M_1 = 0$ . The reacting flow shows a similar qualitative trend. Heat release seems to reduce the compressibility effect even more in confined flows; the ratio of the maximum amplification at  $M_1 = 8$  to that at  $M_1 = 0$  is about two, which is half of the ratio in the nonreacting flow.

Figure 9 shows the effect of heat release on the maximum amplification rate of unstable modes for low-speed ( $M_1 = 1$ ) and high-speed ( $M_1 = 6$ ) flows. In the low-speed flow, the walls make little difference. Heat release stabilizes the low-speed flow; the maximum amplification rate for  $T_{ad} = 8$  is about 15% of the cold flow value. At  $M_1 = 6$ , the confined flows are more unstable than the unconfined flows. The change of the maximum growth rate with Mach number is

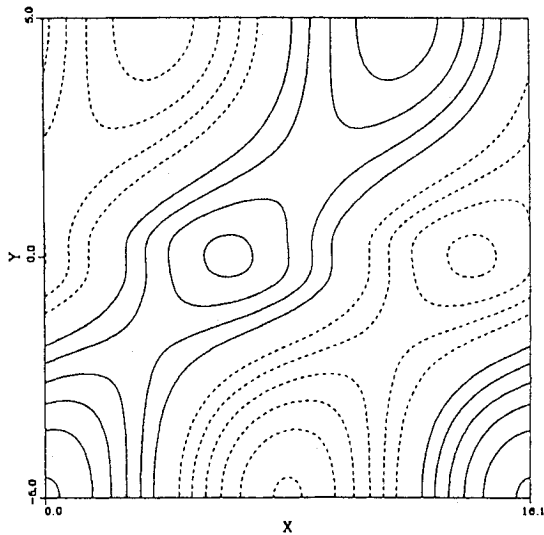


Fig. 10 Pressure contour plots from linear eigenfunctions of the nonreacting confined flow (center mode, max = 1.122, min = 0.878);  $M_1 = 6$  ( $M_2 = 3$ ),  $\bar{T}_2 = 1$ ,  $T_{ad} = 1$ ,  $m = 0$ ,  $H = 5$ .

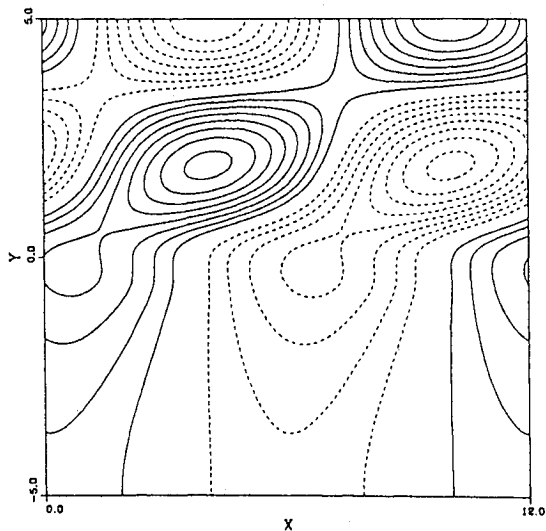


Fig. 11 Pressure contour plots from linear eigenfunctions of the nonreacting confined flow (slow mode, max = 1.167, min = 0.833);  $M_1 = 6$  ( $M_2 = 3$ ),  $\bar{T}_2 = 1$ ,  $T_{ad} = 1$ ,  $m = 0$ ,  $H = 5$ .

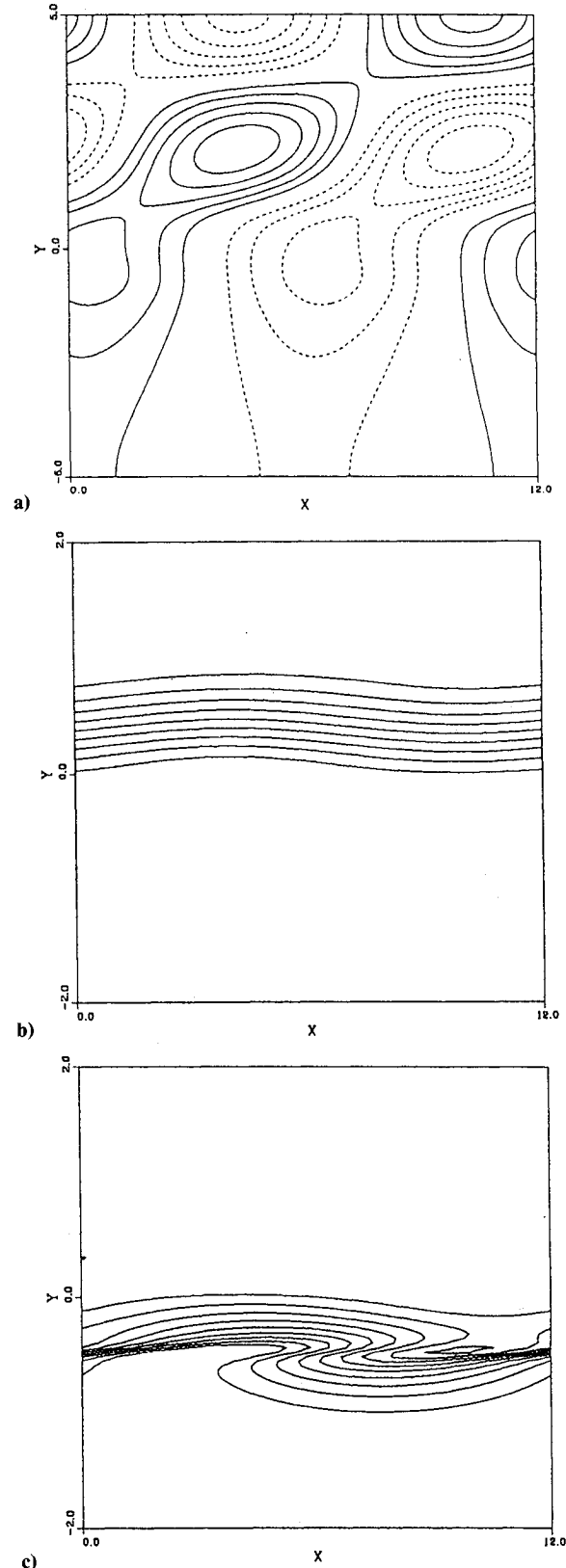


Fig. 12 Contour plots from linear eigenfunctions of the reacting confined flow (slow mode): a) pressure (max = 1.116, min = 0.884), b) fuel (max = 1.0, min = 0.0), and c) oxidizer (max = 1.0, min = 0.0);  $M_1 = 6$  ( $M_2 = 3$ ),  $\bar{T}_2 = 1$ ,  $T_{ad} = 4$ ,  $m = 0$ ,  $H = 5$ .

large in cold flow ( $T_{ad} = 1$ ); it becomes smaller as the heat release increases. The effect of the walls on the growth rate becomes negligible at large heat release. At high Mach numbers, the amplification rates change little with  $T_{ad}$ , which is

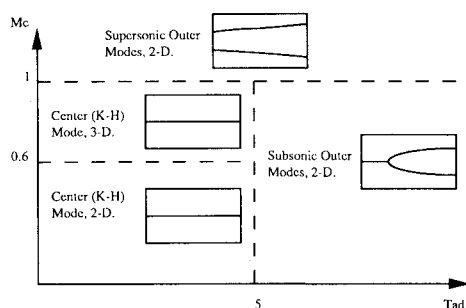


Fig. 13 Dominant unstable modes with their phase speeds.

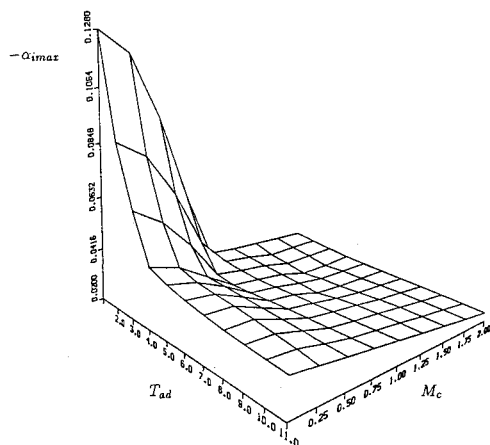


Fig. 14 Maximum growth rates.

consistent with the behavior of the supersonic-ramjet combustor.<sup>17</sup>

#### D. Eigenfunctions

This section studies contours of the flow variables derived from the most unstable eigenfunctions and the mean flow. The eigenfunctions are normalized so that the maximum absolute value of  $\hat{u}$  is unity. We chose  $H = 5$  to include the effect of confinement. We considered only the center and slow modes; the fast mode can be obtained by reflection of the slow mode.

Figure 10 shows the pressure contours produced by the supersonic center mode for the nonreacting ( $T_{ad} = 1$ ) flow at  $M_1 = 6$  ( $M_2 = 3$ ). The pressure contours show clearly the radiative nature of the supersonic center mode. Unlike the outer modes that radiate only to one freestream, the center modes are supersonic relative to both streams, and the associated compression (solid line) and expansion waves (dashed line) propagate toward both boundaries. The patterns of compression/expansion waves in Fig. 10 suggest that the waves are reflected by the walls. The reflections carry energy back to the shear layer, producing feedback that makes confined shear layers more unstable than free shear layers. Mack reported a similar observation for boundary layers.<sup>12</sup>

From the pressure contours, we measured the Mach angle  $\mu$  and estimated the convective Mach number  $M_c$  based on the most unstable mode<sup>10,18</sup> from

$$M_c = 1/\sin \mu \quad (6)$$

Measurement of the Mach angle from Fig. 10 gives about  $\mu = 40$  deg, from which we estimate the convective Mach number to be approximately 1.55. The convective Mach number based on the phase velocity of the most unstable mode is 1.49; this agreement is considered to be very good.

Figures 11 and 12 show contours of nonreacting and reacting supersonic slow modes at  $M_1 = 6$  ( $M_2 = 3$ ). The pressure

contours again show reflections of compression/expansion waves propagating at Mach angle  $\mu = 27$  deg for the nonreacting flow and  $\mu = 26$  for the reacting flow. The convective Mach numbers according to Eq. (6) are 2.20 for the nonreacting flow and 2.28 for the reacting flow, whereas the convective Mach numbers based on the corresponding most unstable modes are 2.22 and 2.33, respectively; the agreement is again very good. The contours of the reactant concentrations in Figs. 12b and 12c show that the slow mode principally affects the oxidizer because the oxidizer occupies the lower part of the layer, leaving the fuel mostly undisturbed. The reverse is true for the fast mode. Thus, the supersonic outer modes will not yield much mixing between the fuel and oxidizer in confined reacting flows.

#### IV. Conclusions

In this work we considered the inviscid stability of the confined compressible reacting mixing layer using laminar-flow profiles generated from solutions of the compressible boundary-layer equations with finite rate chemistry. We found that reflection of supersonic disturbances by the walls makes the mixing layer more unstable than the unconfined free shear layer. Decreasing the distance between the walls makes the flow more unstable. Subsonic disturbances are relatively unaffected by the walls. The most unstable supersonic disturbances are two-dimensional in rectangular channel flows, but three-dimensional in partially confined flows. Heat release and Mach number hardly change the maximum growth rates of supersonic disturbances. The growth rate of the supersonic mixing layer is very small compared to the corresponding incompressible mixing layer value. The supersonic center mode radiates into both boundaries, whereas the outer modes propagate only to one boundary with respect to which they are supersonic. Pressure contours show the reflection of compression/expansion waves that propagate at the Mach angle. The reactants are not strongly mixed by supersonic instabilities because they disturb mainly one side of the layer. Finally, for reference, Fig. 13 shows the diagram of the most dominant unstable modes with their phase speeds in the isentropic convective Mach number and adiabatic flame temperature plane, and Fig. 14 shows the corresponding maximum growth rates.

#### Acknowledgment

This work was sponsored by the Stanford-NASA Center for Turbulence Research.

#### References

- Groppengiesser, H., "Study on the Stability of Boundary Layers in Compressible Fluids," NASA TT F-12, 786, Feb. 1970.
- Sandham, N. D., and Reynolds, W. C., "A Numerical Investigation of the Compressible Mixing Layer," Dept. of Mechanical Engineering, Stanford Univ., TF-45, Stanford, CA, Sept. 1989.
- Jackson, T. L., and Grosch, C. E., "Inviscid Spatial Stability of a Compressible Mixing Layer," *Journal of Fluid Mechanics*, Vol. 208, Nov. 1989, pp. 609-637.
- Jackson, T. L., and Grosch, C. E., "Inviscid Spatial Stability of a Compressible Mixing Layer. Part 2. The Flame Sheet Model," *Journal of Fluid Mechanics*, Vol. 217, Aug. 1990, pp. 391-420.
- Shin, D. S., and Ferziger, J. H., "Linear Stability of the Reacting Mixing Layer," *AIAA Journal*, Vol. 29, No. 10, 1991, pp. 1634-1642.
- Shin, D. S., and Ferziger, J. H., "Stability of Compressible Reacting Mixing Layer," AIAA Paper 91-0372, Jan. 1991.
- Tam, K. W., and Hu, F. Q., "The Instability and Acoustic Wave Modes of Supersonic Mixing Layers Inside a Rectangular Channel," *Journal of Fluid Mechanics*, Vol. 203, June 1989, pp. 51-76.
- Greenough, J., Riley, J., Soestrisno, M., and Eberhardt, D., "The Effect of Walls on a Compressible Mixing Layer," AIAA Paper 89-0372, Jan. 1989.
- Morris, P. J., and Giridharan, M. G., "The Effect of Walls on Instability Waves in Supersonic Shear Layers," *Physics of Fluids*, Vol. 3, Feb. 1991, pp. 356-358.
- Zhuang, M., Dimotakis, P. E., and Kubota, T., "The Effect of Walls on a Spatially Growing Supersonic Shear Layer," *Physics of Fluids*, Vol. 2, April 1990, pp. 599-604.

<sup>11</sup>Shin, D. S., and Ferziger, J. H., "Stability of the Compressible Reacting Mixing Layer," Dept. of Mechanical Engineering, Stanford Univ., TF-53, Stanford, CA, March 1992.

<sup>12</sup>Mack, L. M., "Boundary-Layer Linear Stability Theory," *Special Course on Stability and Transition of Laminar Flow*, AGARD Rept., Vol. 709, 1984, pp. 3-1-3-81.

<sup>13</sup>Papamoschou, D., "Structure of the Compressible Shear Layers," AIAA Paper 89-0126, Jan. 1989.

<sup>14</sup>Clemens, N. T., and Mungal, M. G., "Two- and Three-Dimensional Effects in the Supersonic Mixing Layer," *AIAA Journal*, Vol. 30, No. 4, 1992, pp. 973-981.

<sup>15</sup>Hall, J. L., Dimotakis, P. E., and Rosemann, H., "Some Measurement of Molecular Mixing in Compressible Turbulent Shear Layers," AIAA Paper 91-1719, Jan. 1991.

<sup>16</sup>Papamoschou, D., and Roshko, A., "The Compressible Turbulent Shear Layer: an Experimental Study," *Journal of Fluid Mechanics*, Vol. 197, Dec. 1988, pp. 453-477.

<sup>17</sup>Drummond, P., private communication, NASA Langley Research Center, Hampton, VA, Aug. 1991.

<sup>18</sup>Mack, L. M., "Stability and the Problem of Supersonic Boundary-Layer Transition," *AIAA Journal*, Vol. 13, No. 3, 1975, pp. 278-289.

Recommended Reading from Progress in Astronautics and Aeronautics

## Viscous Drag Reduction in Boundary Layers

*Dennis M. Bushnell and Jerry N. Hefner, editors*

This volume's authoritative coverage of viscous drag reduction issues is divided into four major categories: Laminar Flow Control, Passive Turbulent Drag Reduction, Active Turbulent Drag Reduction, and Interactive Turbulent Drag Reduction. It is a timely publication, including discussion of emerging technologies such as

the use of surfactants as an alternative to polymers, the NASA Laminar Flow Control Program, and riblet application to transport aircraft. Includes more than 900 references, 260 tables and figures, and 152 equations.

1990, 530 pp, illus, Hardback • ISBN 0-930403-66-5  
AIAA Members \$59.95 • Nonmembers \$75.95 • Order #: V-123 (830)

Place your order today! Call 1-800/682-AIAA



American Institute of Aeronautics and Astronautics  
Publications Customer Service, 9 Jay Gould Ct., P.O. Box 753, Waldorf, MD 20604  
Phone 301/645-5643, Dept. 415, FAX 301/843-0159

Sales Tax: CA residents, 8.25%; DC, 6%. For shipping and handling add \$4.75 for 1-4 books (call for rates for higher quantities). Orders under \$50.00 must be prepaid. Please allow 4 weeks for delivery. Prices are subject to change without notice. Returns will be accepted within 15 days.